ELSEVIER

Available online at www.sciencedirect.com

SCIENCE DIRECT®

Organic Electronics 5 (2004) 99–105

Organic Electronics

www.elsevier.com/locate/orgel

Time-resolved photoluminescence in α-PTCDA single crystals: evidence for recombination via Frenkel excitons, charge transfer states, and excimers

R. Scholz [a,*], A.Yu. Kobitski [b], I. Vragović [a], H.P. Wagner [c], D.R.T. Zahn [a]

[a] *Institut für Physik, Technische Universität Chemnitz, 09107 Chemnitz, Germany*
[b] *Abteilung Biophysik, Universität Ulm, 89069 Ulm, Germany*
[c] *Department of Physics, University of Cincinnati, Cincinnati, OH 45221, USA*

Received 8 July 2003; received in revised form 1 March 2004; accepted 1 March 2004

Abstract

The radiative recombination channels in α-PTCDA are analysed with time-resolved PL techniques in the 50 ns range between temperatures of $T = 10$ and $T = 300$ K. The resulting PL spectra are interpreted with calculations based on the transfer of Frenkel excitons and with time-dependent density functional theory applied to different deformed geometries of molecular dimers as microscopic models for self-trapped excitons. At low temperature, the lineshape and radiative lifetime of the most important PL channel can be assigned quantitatively to a vertical transition from the indirect minimum of the Frenkel exciton dispersion towards the electronic ground state. In an intermediate regime below about $T = 100$ K, charge transfer states involving an anionic and a cationic molecule dominate the PL spectra. Radiative recombination from an excimer state in a stack geometry has a rather weak temperature dependence, and due to non-radiative quenching of the other PL channels, this excimer PL band predominates above about $T = 200$ K.

---

1. Introduction

In molecular crystals, the optical absorption and the photoluminescence (PL) spectra are determined by intra-molecular electronic excitations and by transfer of excitons between different molecular sites. Moreover, due to the small intermolecular separation, completely different types of optical excitations like charge transfer (CT) excitons can appear. PTCDA (3,4,9,10-perylene-tetracarboxylic-dianhydride), a reference material among the crystalline organic semiconductors, has served as a model system for various experimental investigations [1] and for the development of microscopic approaches describing the spectroscopic properties.

The Frenkel exciton models for organic crystals can be traced back to the classical work by Davydov [2], and subsequently these methods have been applied in great detail to crystals with small dipole–dipole interactions like anthracene [3]. Initially, the concept of CT states was developed for collective excitations of a linear chain of identical

---

[*] Corresponding author. Tel.: +49-371-531-3145; fax: +49-371-531-3151.
E-mail address: scholz@physik.tu-chemnitz.de (R. Scholz).

1566-1199/$ - see front matter © 2004 Elsevier B.V. All rights reserved.
doi:10.1016/j.orgel.2004.03.001

molecules [4] and stacked donor–acceptor crystals [5,6]. In the case of a crystal of identical molecules, their energetic position defines the onset of charge separation between neighbouring sites, converging to the charge transport gap for very large separations of the charged molecular sites. Self-trapped excitons (STE) have been suggested several times as candidates for strongly red-shifted photoluminescence (PL) bands of crystalline polyacenes [7,8] and other aromatic systems like perylene [9], but attempts to gain quantitative insight into the configuration coordinate diagrams remained phenomenological [9,10].

Concerning the spectroscopic properties of PTCDA, most theoretical investigations have concentrated on the linear optical response, including exciton models adapted from inorganic semiconductors [1], and Frenkel–CT models applied to molecular dimers [11] and a single one-dimensional stack [12,13]. As the CT excitons have only a minor influence on the absorption coefficient, a pure Frenkel exciton model can be used for a quantitative description of the anisotropic dielectric tensor [14], but for modeling electro-absorption the CT states seem to be crucial [15].

In the present work, we propose time-resolved photoluminescence (PL) as an alternative route to gain insight into the energetics of the relaxed excited states of crystalline PTCDA in the α-phase. The strongest low-temperature PL channel can be modeled quantitatively with a Frenkel exciton approach [16–18]. The PL bands with longer radiative lifetime are assigned to localized STE, and explicit microscopic models are proposed based on time-dependent density functional calculations of several deformed molecular dimers resembling the crystalline geometry [16,19].

2. Experimental

Previous PL studies of PTCDA have revealed a large variety of lineshapes [20–24], depending both on details of the sample preparation and the temperature. In amorphous samples, the PL decay becomes faster with respect to dissolved monomers [25], whereas poly-crystalline films show the opposite behaviour [20,22,24]. Therefore, long radiative lifetimes can be interpreted as a signature of the crystalline phase, and it was demonstrated that at low temperature the radiative recombination channels in α-PTCDA single crystals may have lifetimes exceeding 30 ns [26]. The experimental part of the present work extends this study to the temperature range $T = 10$ to 300 K.

The α-PTCDA crystals used in the present investigation were grown by double sublimation in high vacuum. For the time-resolved PL measurements, they were excited with a pulsed dye laser resulting in 20 ps pulses at an energy of 2.19 eV (565 nm). In order to allow for the detection of PL channels with slow radiative decay rates, the repetition rate of 80 MHz was reduced to 4 MHz using a cavity dumper. The time-resolved PL was analysed using a CROMEX 250IS imaging spectrograph and detected by a Hamamatsu C4334 Streakscope with a time resolution better than 50 ps. In order to protect the streakscope against stray light from the laser, a filter with a cutoff at 590 nm (2.10 eV) was used. The low-temperature measurements were performed in a closed-cycle He cryostat.

The transient PL data measured over a temperature range of 10 to 300 K were recorded from about 5 ns before the laser pulse to 45 ns after the excitation, revealing an intensity maximum around $T = 40$ K. As shown in Fig. 1, the vibronic subbands at low temperatures evolve into a structureless PL spectrum at higher temperatures. From a careful data analysis, we conclude that the PL spectra contain six components with different decay times and lineshapes [27]. The model lineshape of the PL channel dominating at low temperatures was based on the measured lineshape at $T = 11$ K [26], allowing however for a linear temperature dependence of the subband position and an increase of the subband broadening with rising temperature [27]. Concerning the other three prominent PL channels, the resulting lineshapes are modeled with a vibronic progression over the vibronic levels of an effective internal mode with $\hbar\omega = 0.16$ eV. In each case, the elongation of this effective mode in the relaxed excited state is in reasonable agreement with the configuration coordinate diagrams discussed in Section 4. Furthermore, we found evidence for two

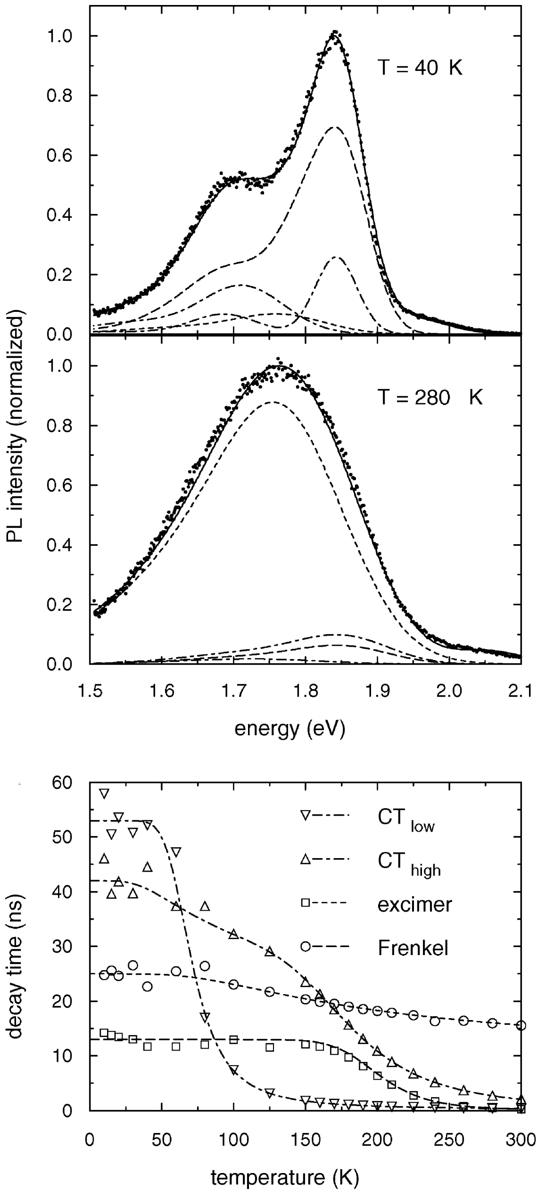

Fig. 1. Upper: Decomposition of the measured time-integrated PL spectra (dots) at $T = 40$ K and $T = 280$ K into contributions from Frenkel excitons (long-dashed), excimers (short-dashed), and two CT channels (dash-dotted), including a high-energy band at 1.95 eV at $T = 40$ K and 2.05 eV at $T = 280$ K (not shown). Lower: Temperature dependence of the decay times of the different PL channels.

types of high-energy satellites, both restricted to a certain temperature range [27].

At $T = 40$ K, the most prominent PL band with a decay time of 12 ns can be reproduced with a model based on Frenkel excitons [17,18], cf. Section 3. The two slowest recombination channels are assigned to CT transitions between two oppositely charged molecules in different deformed dimer geometries [16], cf. Section 4, whereas the fourth channel decaying within about 25 ns is assigned to an excimer in a stack geometry. At $T = 280$ K, the PL due to Frenkel excitons and recombination between ionic pairs is strongly quenched, and instead the excimer band has become the dominant recombination channel, decaying within about 20 ns. In this temperature regime, the high-energy satellite occurring at low temperatures around 1.95 eV is completely quenched, and instead a PL band around 2.05 eV develops.

The temperature-dependent lifetimes of the different PL bands shown in Fig. 1 are calculated using $\tau_{\mathrm{rad}} = (13 \pm 2)$ ns for the Frenkel exciton, (42 ± 6) ns for the high-energy CT band around $\langle E_{\mathrm{PL}} \rangle = 1.78$ eV, (53 ± 6) ns for the low-energy CT band around $\langle E_{\mathrm{PL}} \rangle = 1.67$ eV, and (25 ± 3) ns for the PL arising from the stacked excimer with $\langle E_{\mathrm{PL}} \rangle = 1.72$ eV, and different energy barriers for activated non-radiative decay [27]. Furthermore, at low temperatures, the intensities of the PL channels assigned to different molecular dimers are suppressed due to small energetic barriers for the formation of their precursor states, resulting in a decrease of the overall PL intensity below about $T = 40$ K [27].

3. Optical cycle of Frenkel excitons

After photon absorption at the Γ point of the Brillouin zone, the Frenkel excitons are scattered to the minimum of their dispersion at the surface of the Brillouin zone, cf. Fig. 2. As the electronic and vibronic ground state has vanishing momentum, it cannot be reached by a vertical radiative PL transition starting from this excitonic state at finite wave vector. Therefore, the lowest available state after recombination is the first vibronic level of an effective internal mode, with a wave vector coinciding with the one of the Frenkel exciton

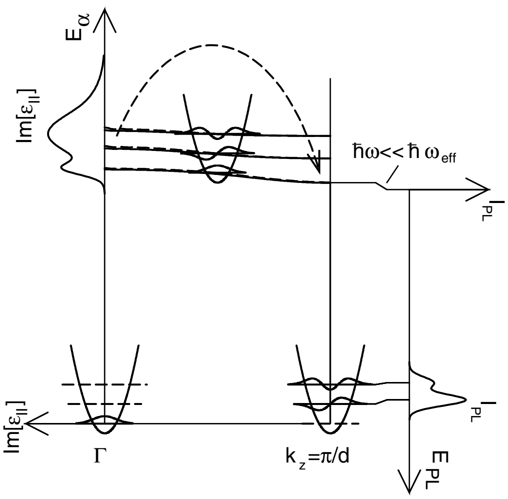

Fig. 2. Schematic model of the optical excitation and recombination cycle in crystalline PTCDA at low temperature. The lineshape observed in optical absorption is visualized as $\mathrm{Im}[\epsilon_{\|}]$ as a function of the energy E_α measured with respect to the ground state at Γ, and the origin of the PL energy scale E_{PL} is related to the lowest relaxed excited state available. For the exciton dispersion branches, their relation to the vibronic levels of an excited molecule is visualized for $k_z = \frac{\pi}{2d}$ where the dominating influence of the stack neighbours on the dispersion vanishes. Vibronic levels v_g not involved in the absorption and PL transitions are visualized as dashed lines.

before radiative recombination. In a Frenkel exciton model including an effective internal mode at 0.17 eV, the overall Stokes shift between the lowest vibronic subband in absorption at 2.23 eV and the highest subband of the Frenkel exciton PL at 1.82 eV can be decomposed into contributions from the exciton dispersion (0.12 eV), the lack of the lowest vibronic state after recombination (0.17 eV), correlation of the final states after recombination (0.035 eV), and internal vibrations with frequencies far below the effective mode (0.085 eV) [17,18].

In Fig. 3, we compare the lineshapes calculated with the Frenkel exciton model [14,17,18] with the observed absorption of thin films [28] and the most prominent PL channel at low temperature [26]. Each vibronic subband was modeled with an asymmetric lineshape based on a Poisson progression for a low-frequency internal mode [18]. The calculated radiative lifetime of 13 ns coincides with the measured decay time of this PL channel at low temperatures, 13 ± 2 ns, cf. Section 2.

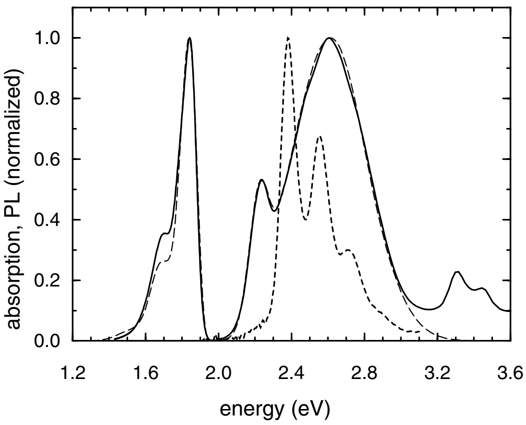

Fig. 3. Comparison of the calculated absorption [14] and PL [17,18] lineshapes (dashed lines) with the experimental absorption coefficient of poly-crystalline thin films [28] and the dominating PL band at low temperature [26] (solid lines). The absorption of dissolved PTCDA molecules [13] is shown for comparison (short-dashed line).

4. Charge transfer transitions in self-trapped dimer states

All calculations discussed in the present section have been performed with the time-dependent density functional (TD-DFT) scheme based on the B3LYP functional as implemented in the GAUSSIAN98 package. The choice of the relatively small 3-21G basis set was motivated by the need to apply precisely the same approach both to PTCDA monomers and dimers. For the dimers this was the largest possible basis set which could be run on the HP-9000 N4000 hardware used, and each dimer geometry took between 40 and 90 h on a single processor of this system, resulting in a total CPU time of about five months for all the 70 dimer geometries investigated.

The model geometries are based on the atomic positions in the crystal unit cell determined by X-ray diffraction [29], and the positions of the hydrogen atoms have been readjusted with a calculation of the 3-dim unit cell applying density functional tight-binding techniques [30,31]. Energy offsets related to the variational basis set and to the quantum chemical method used have been eliminated by comparing the calculated transition energies for a molecule in a geometry compatible with the so-defined α-PTCDA crystal with a relaxed free molecule, the transition energies measured for PTCDA monomers in superfluid He [32], and with the molecular transition energy required in exciton models for the crystalline phase [14]. Two kinds of deformed dimers have been investigated: anion–cation pairs and excimer states, where the molecules are deformed as in the relaxed excited state of the monomer [30]. In both cases, the prefactor of the overall deformation has been varied in 20% steps between the crystal reference geometry and the largest deformation applied, corresponding to the ionic geometry for the anion–cation pairs and to half of the deformation in the relaxed excited state for each molecule in the pair forming the excimer. It turned out that the minimum of the excimer energy occurs around 45% of the deformation of the relaxed excited monomer, whereas the minimum towards the anion–cation pair is close to the expected deformation of the ionic pair.

The dimer geometries investigated include pairs of the same basis molecule displaced along the **a** or **b** lattice vectors of α-PTCDA, a dimer of the two coplanar basis molecules in the unit cell, and two further non-coplanar dimers involving both kinds of basis molecules. In each case, we have performed a careful adjustment of the overall energy scale due to the lack of the crystal surroundings, where a molecular transition energy of 2.35 eV in crystalline α-PTCDA [14] has served as a guideline.

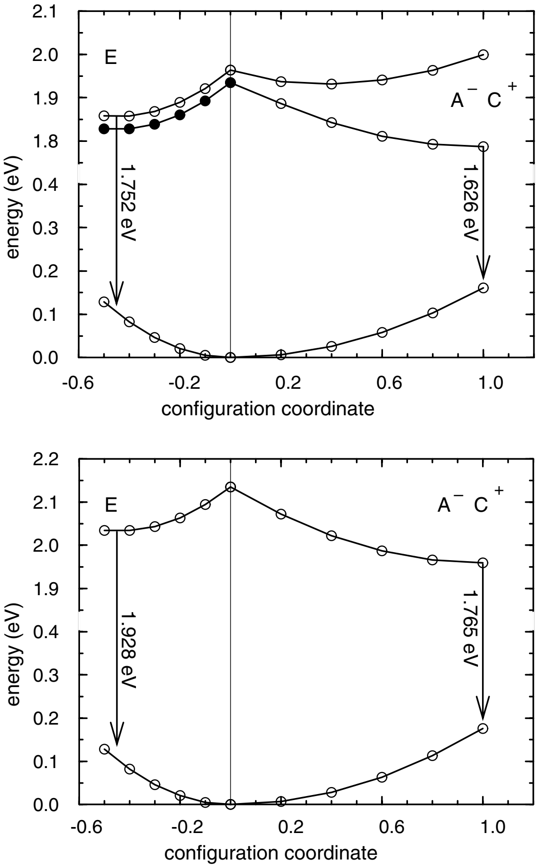

Fig. 4. Upper: Configuration coordinate diagram for a stack dimer, where the deformation of the excimer towards the left is compatible with the relaxed excited state of the monomer, and the deformation towards the right with an anion–cation (A^-C^+) pair. For the excimer (*E*), the higher transition is dipole-allowed, while the lower transition is forbidden by parity. The arrows indicate the energies of radiative recombination from the minimum of the excited state surface. Lower: Configuration coordinate diagram for a pair of non-coplanar molecules of different orientation, with a distance of 10.5 Å between their centers of mass.

In Fig. 4, we report two typical configuration coordinate diagrams for molecular dimers: the stack geometry, and a dimer consisting of two inequivalent molecules belonging to two consecutive molecular planes in the crystal. From the minima of the excited states in the stack geometries investigated, we assign the observed low-energy CT band with $\langle E_{\mathrm{PL}} \rangle = 1.67$ eV to the transition energy of 1.626 eV in the anion–cation stack, while the excimer PL band with $\langle E_{\mathrm{PL}} \rangle = 1.72$ eV dominating at high temperatures can be related to the transition energy of 1.752 eV for an excimer in a stacked geometry. From the transition energies calculated for the dimer involving the two different non-coplanar basis molecules, we assign the observed average of $\langle E_{\mathrm{PL}} \rangle = 1.78$ eV to the CT recombination between an anion and a cation at 1.765 eV in the configuration coordinate diagram. The energetic minimum in the excimer geometry determines a transition energy of 1.928 eV, a candidate for the slow component of the high-energy satellite around 1.95 eV in the low-temperature PL spectra.

The agreement between the calculated transition energies for the deformed dimers with the positions of the observed PL bands is quite remarkable. As our approach does not account for the Stokes shift resulting from external phonon modes [16,33] and self-trapping along the intermolecular distance, we can use these deficiencies for an estimate of systematic errors of the TD-DFT calculation. From their resonant Raman intensities, we expect the external phonons to contribute 40 meV to the reorganization energy in absorption [16]. The internal deformation of the molecules in the stacked excimer geometry in Fig. 4 results in a Stokes shift half as large as for the monomer [30], so that it is reasonable to assume that the contribution of the librational phonons is reduced by the same amount. The self-trapping of the excimer along the stack distance can be investigated with a combination of configuration interaction of singles and second order Møller-Plesset theory, resulting in a Stokes shift of 0.09 eV [34].

Combining the measured excimer PL around $\langle E_{\mathrm{PL}} \rangle = 1.72$ eV with the three contributions to the Stokes shift, i.e. 0.21 eV for the internal deformations as reported in Fig. 4, 0.04 eV for the librational phonons, and 0.11 eV for the self-trapping along the stack distance, we find an estimate of 2.06 eV for the CT transition along the stack in the geometry of the α-phase, remaining significantly below the CT energies obtained with micro-electrostatic calculations [35,36].

5. Conclusion

We have demonstrated the existence of six distinct radiative recombination channels in α-PTCDA, including four strong bands and two high-energy satellites. The dominating low-temperature PL band was assigned quantitatively to recombination from the dispersion minimum of the Frenkel excitons. With time-dependent density functional calculations, the three PL bands with slower decay times were assigned to different kinds of internally deformed molecules, including two geometries of anion–cation pairs and a stack excimer. From an investigation of the self-trapping of the excimer along the inter-molecular distance, we conclude that the CT transition along the undeformed stack occurs at 2.06 eV, an important ingredient for exciton models of electro-absorption.

References

[1] S.R. Forrest, Chem. Rev. 97 (1997) 1793.

[2] A.S. Davydov, Zh. Eksp. Teor. Fiz. 18 (1948) 210; A.S. Davydov, Theory of Molecular Excitons, Plenum Press, New York, 1971.

[3] L.B. Clark, M.R. Philpott, J. Chem. Phys. 53 (1970) 3790.

[4] J.I. Krugler, C.G. Montgomery, H.M. McConnell, J. Chem. Phys. 41 (1964) 2421.

[5] P.J. Strebel, Z.G. Soos, J. Chem. Phys. 53 (1970) 4077.

[6] D. Haarer, M.R. Philpott, H. Morawitz, J. Chem. Phys. 63 (1975) 5238.

[7] H. Nishimura, T. Yamaoka, A. Matsui, K. Mizuno, G.J. Sloan, J. Phys. Soc. Jpn. 54 (1985) 1627.

[8] K. Furuta, T. Yamada, H. Moriya, K. Mizuno, A.H. Matsui, in: K. Cho, A. Matsui (Eds.), Proceedings of the International Conference on Excitonic Processes in Condensed Matter 2000, World Scientific, Singapore, 2001, p. 185.

[9] H. Nishimura, T. Yamaoka, K. Mizuno, M. Iemura, A. Matsui, J. Phys. Soc. Jpn. 53 (1984) 3999.

[10] T.-M. Wu, D.W. Brown, K. Lindenberg, Phys. Rev. B 47 (1993) 10122.

[11] M.H. Hennessy, Z.G. Soos, R.A. Pascal, A. Girlando, Chem. Phys. 245 (1999) 199.

[12] M.H. Hennessy, R.A. Pascal, Z.G. Soos, Proc. SPIE Int. Soc. Opt. Eng. 3797 (1999) 89.

[13] M. Hoffmann, K. Schmidt, T. Fritz, T. Hasche, V.M. Agranovich, K. Leo, Chem. Phys. 258 (2000) 73.

[14] I. Vragović, R. Scholz, M. Schreiber, Europhys. Lett. 57 (2002) 288.

[15] G. Mazur, P. Petelenz, M. Slawik, J. Chem. Phys. 118 (2003) 1423.

[16] R. Scholz, I. Vragović, A.Yu. Kobitski, G. Salvan, T.U. Kampen, M. Schreiber, D.R.T. Zahn, in: V.M. Agranovich, G.C. La Rocca (Eds.), Proceedings of the International School of Physics "E. Fermi", course CXLIX: Organic nanostructures: Science and applications, IOS Press, Amsterdam, 2002, p. 379.

[17] R. Scholz, I. Vragović, A.Yu. Kobitski, M. Schreiber, H.P. Wagner, D.R.T. Zahn, Phys. Status Solidi. B 234 (2002) 403.

[18] I. Vragović, R. Scholz, Phys. Rev. B 68 (2003) 155202.

[19] R. Scholz, A.Yu. Kobitski, I. Vragović, T.U. Kampen, D.R.T. Zahn, H.-P. Wagner, in: A.R. Long, J.H. Davies (Eds.), Proceedings of the 26th International Conference

on the Physics of Semiconductors, Edinburgh, 29 July–2 August 2002, Institute of Physics Conf. Ser., 171, Institute of Physics Publishing, Bristol, 2002, p. 266.
[20] F.F. So, S.R. Forrest, Phys. Rev. Lett. 66 (1991) 2649.
[21] E.I. Haskal, Z. Shen, P.E. Burrows, S.R. Forrest, Phys. Rev. B 51 (1995) 4449.
[22] V. Bulović, P.E. Burrows, S.R. Forrest, J.A. Cronin, M.E. Thompson, Chem. Phys. 210 (1996) 1.
[23] A. Nollau, M. Hoffmann, K. Floreck, T. Fritz, K. Leo, J. Appl. Phys. 87 (2000) 7802.
[24] A.Yu. Kobitski, G. Salvan, H.P. Wagner, D.R.T. Zahn, Appl. Surf. Sci. 179 (2001) 209.
[25] U. Gómez, M. Leonhardt, H. Port, H.C. Wolf, Chem. Phys. Lett. 268 (1997) 1.
[26] A.Yu. Kobitski, R. Scholz, I. Vragović, H.P. Wagner, D.R.T. Zahn, Phys. Rev. B 66 (2002) 153204.
[27] A.Yu. Kobitski, R. Scholz, D.R.T. Zahn, H.P. Wagner, Phys. Rev. B 68 (2003) 155201.
[28] A. Djurišić, T. Fritz, K. Leo, Opt. Commun. 183 (2000) 123.
[29] A.J. Lovinger, S.R. Forrest, M.L. Kaplan, P.H. Schmidt, T. Venkatesan, J. Appl. Phys. 55 (1984) 476.
[30] R. Scholz, A.Yu. Kobitski, T.U. Kampen, M. Schreiber, D.R.T. Zahn, G. Jungnickel, M. Elstner, M. Sternberg, Th. Frauenheim, Phys. Rev. B 61 (2000) 13659.
[31] R. Scholz, M. Friedrich, G. Salvan, Th. Kampen, D.R.T. Zahn, T. Frauenheim, J. Phys.: Condens. Mat. 15 (2003) S2647.
[32] M. Wewer, F. Stienkemeier, Phys. Rev. B 67 (2003) 125201.
[33] G. Salvan, D.A. Tenne, A. Das, T.U. Kampen, D.R.T. Zahn, Org. Electron. 1 (2000) 49.
[34] R. Scholz et al., in preparation.
[35] G. Mazur, P. Petelenz, Chem. Phys. Lett. 324 (2000) 161.
[36] E.V. Tsiper, Z.G. Soos, Phys. Rev. B 64 (2001) 195124.